Engineering with Computers
DOI 10.1007/s00366-011-0253-7

ORIGINAL ARTICLE

Multilayered thresholding-based blood vessel segmentation for screening of diabetic retinopathy

M. Usman Akram · Shoab A. Khan

Received: 3 May 2011 / Accepted: 23 December 2011

Abstract Diabetic retinopathy screening involves assessment of the retina with attention to a series of indicative features, i.e., blood vessels, optic disk and macula etc. The detection of changes in blood vessel structure and flow due to either vessel narrowing, complete occlusions or neovascularization is of great importance. Blood vessel segmentation is the basic foundation while developing retinal screening systems since vessels serve as one of the main retinal landmark features. This article presents an automated method for enhancement and segmentation of blood vessels in retinal images. We present a method that uses 2-D Gabor wavelet for vessel enhancement due to their ability to enhance directional structures and a new multilayered thresholding technique for accurate vessel segmentation. The strength of proposed segmentation technique is that it performs well for large variations in illumination and even for capturing the thinnest vessels. The system is tested on publicly available retinal images databases of manually labeled images, i.e., DRIVE and STARE. The proposed method for blood vessel segmentation achieves an average accuracy of 94.85% and an average area under the receiver operating characteristic curve of 0.9669. We compare our method with recently published methods and experimental results show that proposed method gives better results.

M. U. Akram (✉)
Computer and Software Engineering Department,
Bahria University, Islamabad, Pakistan
e-mail: usmakram@gmail.com

S. A. Khan
Department of Computer Engineering College of Electrical and Mechanical Engineering, National University of Sciences and Technology, Rawalpindi, Pakistan
e-mail: shoabak@yahoo.com

Keywords Diabetic retinopathy · Blood vessels · Wavelet · Multilayered thresholding

1 Introduction

There is ever-increasing interest in the development of automatic biomedical diagnosis systems due to the advancement in computing technology, to improve the service by medical community and also to help the ophthalmologists. The knowledge about health and disease is required for reliable and accurate medical diagnosis. Digital information is acquired at different scales, quickly and efficiently by means of image processing techniques. So the algorithms can be developed for computer aided medical diagnosis based on image processing technology. Patients with diabetes are more likely to develop eye problems such as cataracts and glaucoma, but the disease's affect on the retina is the main threat to vision [1]. One of the complications of abnormalities in the retina and in the worst case blindness or severe vision loss is called diabetic retinopathy (DR) [1].

Patients may not notice a change in their vision as diabetic retinopathy is often asymptomatic; however, the damage is always irreversible if not caught in a timely fashion [2]. Non-proliferative retinopathy is the less serious form and occurs when an abnormality develops in the retinal capillaries, allowing fluid to leak into the tissue of the eye [3]. In this condition, a network of small blood vessels, called choroidal neovascularization (CNV), arises in the choroid and taking a portion of the blood supplying the retina. As the amount of blood supplying the retina is decreased, the sight may be degraded and in the severe cases blindness may occur [4]. The eye is a window to the retinal vascular system which is uniquely accessible for the

Published online: 05 January 2012

study of a continuous vascular bed in humans [5]. The most common signs of diabetic retinopathy include hemorrhages, cotton wool spots, dilated retinal veins, and hard exudates [6–8].

An essential feature in screening of DR is the appearance of blood vessels in ocular fundus. Retinal images, also known as fundus images, are acquired by making photographs of the back of the eye. We are interested in vessel segmentation for screening of diabetic retinopathy. Eye care specialists can screen vessel abnormalities using an efficient and effective computer-based approach to the automated segmentation of blood vessels in retinal images. The detection and measurement of blood vessels can be used to quantify the severity of disease, as part of the process of automated diagnosis of disease or in the assessment of the progression of therapy [9]. Automated segmentation reduces the time required by a physician or a skilled technician for manual labeling [1]. Thus a reliable method of vessel segmentation would be valuable for the early detection and characterization of changes due to such diseases [9].

Retinal vascular pattern is used for automatic generation of retinal maps for the treatment of age-related macular degeneration [10], extraction of characteristic points of the retinal vasculature for temporal or multimodal image registration [11], retinal image mosaic synthesis, identification of the optic disc position [12], and localization of the fovea [13]. The challenges faced in automated vessel detection include wide range of vessel widths, low contrast with respect to background and appearance of variety of structures in the image including the optic disc, the retinal boundary and other pathologies [14]. Methods based on vessel tracking to obtain the vasculature structure, along with vessel diameters and branching points have been proposed by Liu and Sun [15], Zhou et al. [16], Chutatape et al. [17], Tolias and Panas [18], Can et al. [19] and Lalonde et al. [20]. Tracking is done by following vessel center lines guided by local information. In [21], ridge detection was used to form line elements and partition the image into patches belonging to each line element resulting in generation of pixel features. Many features were presented and a feature selection scheme is used to select those which provide the best class separability. Papers [22–25] used deformable models for vessels segmentation. Chuadhuri et al. [26] proposed a technique using matched filters to emphasize blood vessels. An improved region-based threshold probing of the matched filter response technique was used by Hoover et al. [27]. Soares et al. [28] segmented blood vessels using 2-D Gabor wavelets along with supervised classification.

This article presents the automated vessel enhancement and segmentation technique for colored retinal images. Segmentation of blood vessels from image is a difficult task due to thin vessels and low contrast between vessel edges and background. The proposed method enhances the vascular pattern using 2-D Gabor wavelet and then it uses a new multilayered thresholding technique to generate gray level segmented image. In multilayered thresholding, the proposed method applies different threshold values iteratively. It finds vessel edges and eliminates false edges and small vessel segments iteratively to generate a gray level thresholded image. Finally it applies adaptive thresholding to generate a binary mask for blood vessel segmentation. The accuracy of proposed technique is tested using two publicly available databases, i.e., DRIVE [21] and STARE [27]. We compare our results with Chaudhuri et al. [26], Jiang et al. [29], Staal et al. [21], Soares et al. [28] and Fraz et al. [30]. We also compare Gabor wavelet-based enhancement method with Hoover et al. [27].

This article consists of four sections. Sect. 1 gives an introduction to diabetic retinopathy, how a computer aided system can be useful for screening of DR and explains already presented techniques. Sect. 2 describes the proposed diabetic retinopathy system. A detailed explanation of proposed method is included in this section. The experiments and their results are presented in Sect. 3, followed by conclusion in Sect. 4

2 Proposed technique

Automatically locating the accurate vascular pattern is very important in implementation of vessel screening system. An automated vessel screening system to facilitate the specialists is an application of medical systems. Original retinal image is in RGB color model having an almost empty blue band whereas red band is normally saturated but green channel gives good representation of retinal image features. Furthermore, in inverted green channel, blood vessels appear more lighter than background that is why we have used inverted green channel for blood vessel enhancement and segmentation. 2-D Gabor wavelet is applied on inverted green channel to enhance the vascular pattern, especially, the thin and less visible vessels [31]. After vessel enhancement, multilayered thresholding and adaptive thresholding techniques are applied to create a binary mask for blood vessel segmentation. The blood vessels are marked by the masking procedure which assigns one to all those pixels which belong to blood vessels and zero to non-vessels pixels.

Figure 1 shows the complete flow diagram for proposed technique. It illustrates the step by step results from input retinal image to blood vessel segmentation.

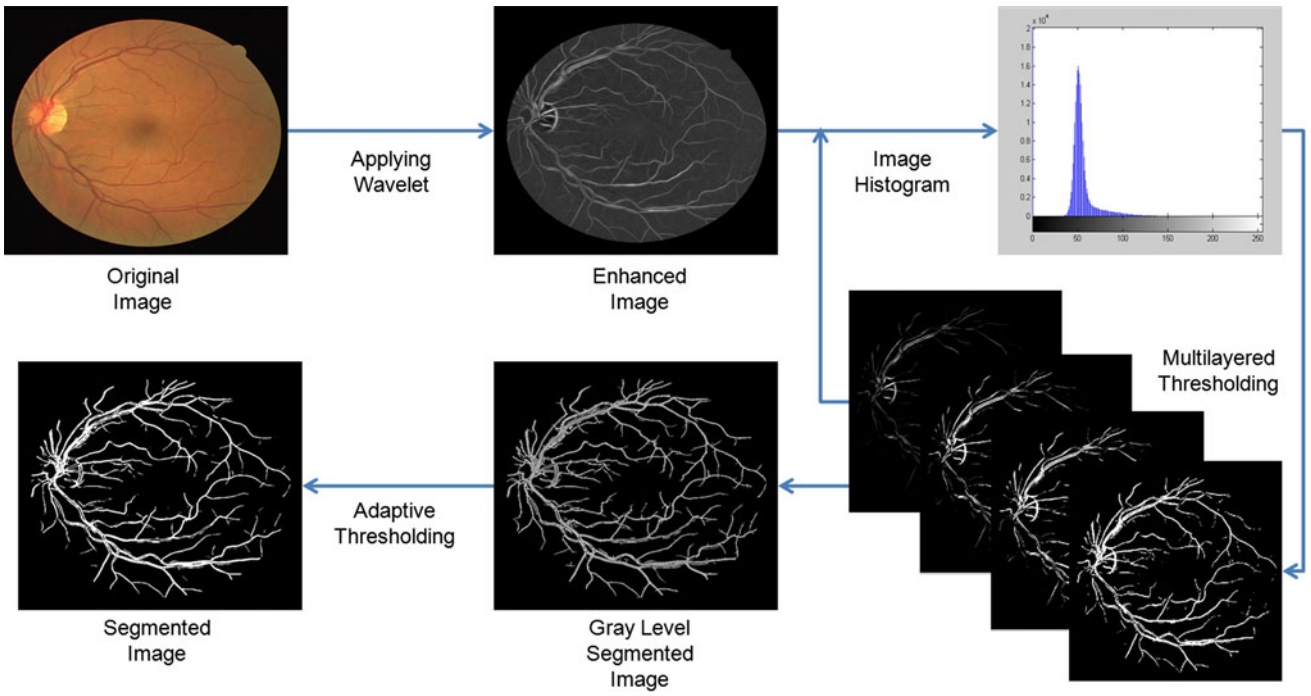

Fig. 1 Complete flow diagram for vessel enhancement and segmentation

2.1 Vessel enhancement

The problem with blood vessel segmentation is that the visibility of vascular pattern is usually not good especially for thin vessels. So, it is necessary to enhance the vascular pattern. Normally matched filters [27] and Gabor filters are used for this purpose but here we have used 2-D Gabor wavelet to enhance the vascular pattern and thin vessels [31]. Gabor wavelets have directional selectiveness capability. They act as low level oriented edge discriminators and also filter out the background noise of the image. Since vessels have directional pattern, so 2-D Gabor wavelet is best option due to its directional selectiveness capability of detecting oriented features and fine tuning to specific frequencies [31].

Let $g(x, y)$ represents the inverted green channel of input colored retinal image and the real plane $\mathcal{R} \times \mathcal{R}$ is denoted as $\mathcal{R}^2$. All 2-D vectors are represented by bold letters, e.g., $\mathbf{x}$, $\mathbf{b}$ and $\mathbf{k}$. We have used 2-D continuous wavelet transform (CWT) instead of 2-D discrete wavelet transform (DWT) due to the rotation operation of 2-D CWT by so-called directional wavelets. The 2-D CWT T_ψ ($\mathbf{b}$, θ, a) is defined in terms of the scalar product of $g(x, y)$ with the transformed wavelet $\psi_{\mathbf{b}}$, θ, $a(\mathbf{x})$ using (1)

$$\begin{aligned} T_\psi(\mathbf{b},\theta,a) &= C_\psi^{-1/2}\langle \psi_{\mathbf{b},\theta,a}|g\rangle \\ &= C_\psi^{-1/2}a^{-1}\int \psi^*_{\mathbf{b},\theta,a}(\mathbf{x})g(x,y)\mathrm{d}^2\mathbf{x}, \end{aligned} \tag{1}$$

where $\mathbf{x} = [xy]^T, g \in \mathcal{R}^2$ is an image represented as a square integrable (i.e., finite energy) function defined over $\mathcal{R}^2$ and $\psi \in \mathcal{R}^2$ be the analyzing wavelet. ψ^* denotes the complex conjugate of ψ. C_ψ, $\mathbf{b}$, θ and a denote the normalizing constant, the displacement vector, the rotation angle, and the dilation parameter, respectively. The analyzing wavelet is defined as

$$\psi_{\mathbf{b},\theta,a}(\mathbf{x}) = a^{-1}\psi(a^{-1}r_{-\theta}(\mathbf{x}-\mathbf{b})), \tag{2}$$

where $a > 0$ and r_θ is the two dimensional rotation along $\mathbf{x}$. It is easy to implement wavelet transform using the Fast Fourier Transform (FFT) algorithm. The vector $\mathbf{x}$ is used to represent the spatial location in the image and $\mathbf{k}$ is associated to a given spatial frequency. FFT of analyzing wavelet ψ is defined as

$$\hat{\psi}_{\mathbf{b},\theta,a}(\mathbf{k}) = a\exp(-j\mathbf{b}\mathbf{k})\hat{\psi}(ar_{-\theta}(\mathbf{k})). \tag{3}$$

The CWT defined in (1) can be written as

$$T_\psi(\mathbf{b},\theta,a) = C_\psi^{-1/2}a\int \exp(j\mathbf{k}\mathbf{b})\hat{\psi}^*(ar_{-\theta}\mathbf{k})\hat{g}(\mathbf{k})\mathrm{d}^2\mathbf{k}, \tag{4}$$

where $j = \sqrt{-1}$, and the hat ($\hat{\psi}^*$ and $\hat{g}$) denotes a Fourier transform.

The 2-D Gabor wavelet also known as Morlet wavelet is defined as [31]

$$\psi_G(\mathbf{x}) = \exp(j\mathbf{k}_0\mathbf{x})\exp\left(-\frac{1}{2}|\mathbf{A}\mathbf{x}|^2\right), \tag{5}$$

$$\hat{\psi}_G(\mathbf{x}) = (\det B)^{1/2} \exp\left(-\frac{1}{2}(B(\mathbf{k}-\mathbf{k}_0)^2)\right), \quad (6)$$

where $\mathbf{k}_0 \in \mathcal{R}^2$ is a vector that defines the frequency of the complex exponential, $B = A^{-1}$ and $A = \begin{bmatrix} \epsilon^{-1/2} & 0 \\ 0 & 1 \end{bmatrix}$ with elongation $\varepsilon \geq 1$ is a 2×2 positive definite diagonal matrix which defines the wavelet anisotropy and elongation of filter in any desired direction. For each pixel position and considered scale value, the Gabor wavelet transform $M_\psi(\mathbf{b}, a)$ is computed for θ spanning from 0° up to 165° at steps of 15° and the maximum is taken.

$$M_\psi(\mathbf{b}, a) = \max|T_\psi(\mathbf{b}, \theta, a)|. \quad (7)$$

In this way by tuning Gabor wavelet to a suitable frequency, for each pixel position, orientation and scale, strong wavelet response R_{wavelet} is kept as a blood vessel. We applied Gabor wavelet on both databases by tuning its parameters. Table 1 shows the selected values for each parameter.

Figure 2 shows the results of vessel enhancement using STARE database. It shows a comparison between matched filter-based [27] and Gabor wavelet-based vessel enhancement methods. Wavelet response gives better results especially for thin vessels.

2.2 Multilayered thresholding

In this article we propose a new multilayered thresholding technique for blood vessel segmentation which takes wavelet response as an input. Wavelet-based enhanced image has larger values of R_{wavelet} where vessels are wide and prominent whereas R_{wavelet} is low in case of thin vessels and edge pixels. Figure 3 shows enhanced retinal image and enlarged blood vessels to show wavelet response R_{wavelet} in detail.

It is clear from the figure that blood vessels have high response at center and low on edges and for thin vessels. So it is very difficult to find one optimal threshold value for accurate blood vessel segmentation without any supervised algorithm. In our multilayered thresholding technique, we apply different thresholds values iteratively and keep track of vessels in successive layers. At the start of segmentation, initial threshold value T_{max} is selected using histogram of R_{wavelet} such that it only keeps those pixels in initial

Table 1 Parameter values for Gabor wavelet

Parameter	Value
Dilation (a)	3
Elongation (ϵ)	4
Rotation angle (θ)	15°
$\mathbf{k}_0$	[0, 3]

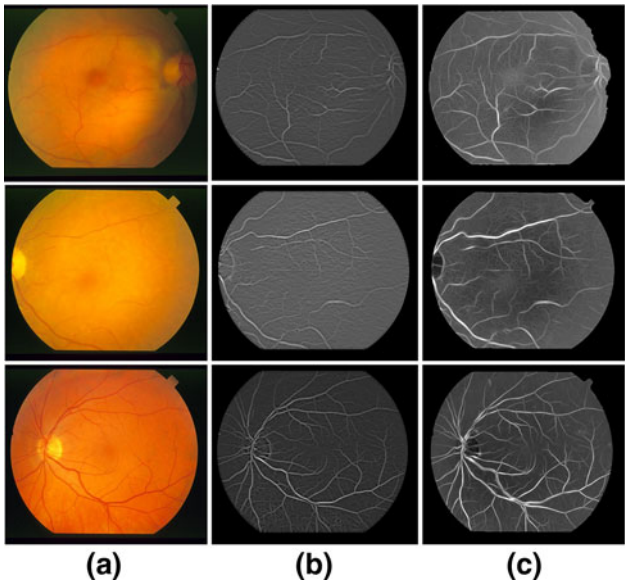

Fig. 2 Blood vessel enhancement: **a** original images, **b** matched filter response and **c** Gabor wavelet response

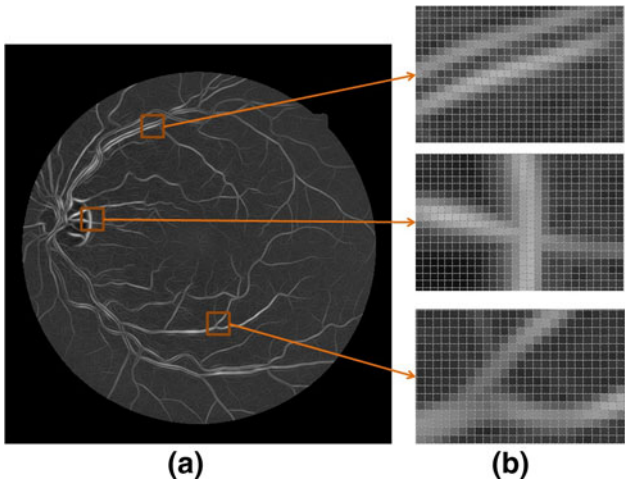

Fig. 3 **a** Enhanced retinal image and **b** enlarged blood vessels

segmented image $I_{\text{segmented}}$ for which R_{wavelet} are higher than T_{max}. The segmented image $I_{\text{segmented}}$ is then skeletonized I_{thin} using thinning morphological operator given in [32] as a result of which all vessels are now only one pixel wide. In order to track the segmented blood vessels, edge image I_{edge} highlighting edge pixels of all vessels is computed using equation . For every pixel p in I_{thin}

$$\text{Edge}(p) = \frac{1}{2}\sum_{i=1}^{8} |I_{\text{thin}}(p_{\text{imod8}}) - I_{\text{thin}}(p_{i-1})| \quad (8)$$

Where p_0 to p_7 are the pixels belonging to an clockwise ordered sequence of pixels defining the 8-neighborhood of p and $I_{\text{thin}}(p)$ is the pixel value. $I_{\text{thin}}(p) = 1$ for vessel pixels and zero elsewhere. Edge$(p) = 1$ and Edge$(p) = 2$ correspond to vessel edge point and intermediate vessel

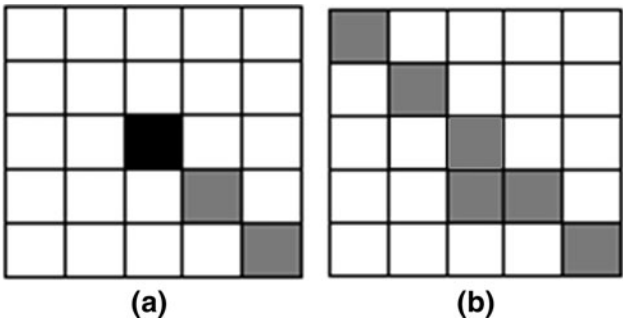

Fig. 4 Vessel edge detection. **a** Vessel edge pixel (*black pixel*) with Edge(p) = 1. **b** Intermediate vessel pixels (*gray pixels*) with Edge(p) = 2

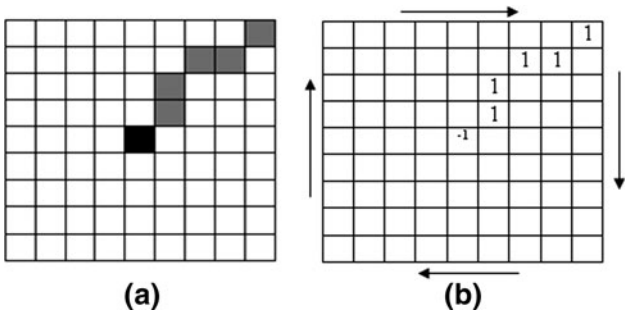

Fig. 5 Validation of vessel edge pixels: **a** vessel segment containing vessel edge pixel (*black pixel*), **b** tracking blood vessel for edge validation

point, respectively. Figure 4 shows a vessel edge pixel (black pixel) and intermediate pixels (gray pixels). The vessel edges obtained from this algorithm must be filtered to preserve only the true edges. In order to eliminate false edges due to break in vessel and small segments from I_{edge}, take a window of size $w \times w$ and place the vessel edge point at the center of window. If there exists another edge point within the window then remove both of them as they occurred due to a break in vessel. In order to remove small segments, track the vessel from edge point and if another edge is detected within the window remove those segments. Figures 5 and 6 shows elimination of false vessel edges, removal of short segments and validation of true vessels edges.

Initialize difference image I_{diff} and segmented vessel image I_{vessel} with I_{edge}. Reduce the threshold value by 1 and calculate $I_{\text{segmented}}$ for next iteration.

Following steps are then performed iteratively:

1. Compute I^j_{thin} using segmented image $I^i_{\text{segmented}}$ for jth iteration where $i < j$.
2. Find out edge image I^j_{edge} by removing false edges, small segments and validating the edges.
3. Calculate $I^j_{\text{diff}}(x, y) = I^j_{\text{edge}} - I^i_{\text{edge}}$ where $i < j$. Only keep those pixels in I_{diff} which are connected to vessel edge pixels in I_{edge}. If new added vessel segments are more than 10 pixels add them in I_{vessel}.
4. If $I^j_{\text{vessel}} - I^i_{\text{vessel}} = 0$, stop iteration otherwise set $T_{\max} = T_{\max} - 1$ and calculate $I^j_{\text{segmented}}$.

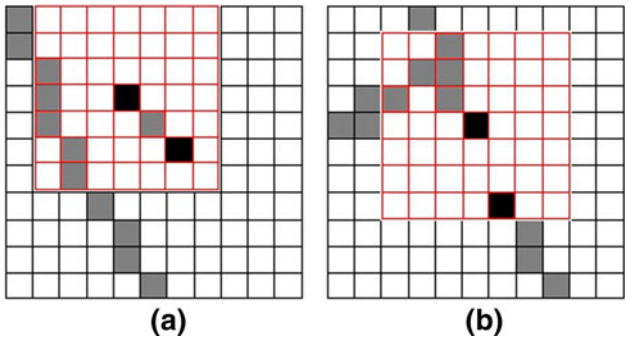

Fig. 6 Elimination of false edges: **a** false edges due to small vessel segments, **b** false edges due to vessel breakage

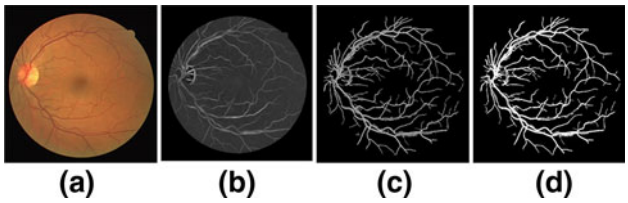

Fig. 7 Multilayered thresholding: **a** input retinal image; **b** wavelet-based enhanced vascular pattern; **c** multilayered thresholding output; **d** adaptive threshold-based vessel segmentation mask

Final segmented image $I_{\text{segmented}}$ is used to create a gray level segmented image which contains selected blood vessels only with their original intensity values. An adaptive threshold is further applied to improve the segmentation accuracy and to generate a binary mask for blood vessel segmentation. Figure 7 shows the gray level segmented vessels and final binary segmentation mask after applying adaptive thresholding technique [32].

3 Results

In medical imaging diagnosis systems, the accuracy of result is very critical; that is why we have used two databases DRIVE [21] and STARE [27] to check the vessel segmentation accuracy. The DRIVE database has been collected by Hoover et al. [27] and it consists of 40 RGB color images of the retina seven of which contain different pathologies. The images are taken digitally from a Canon CR5 3CCD camera with 45° field of view(FOV) and images are of size 768 × 584 pixels, 8 bits per color channel. The STARE database consists of 20 RGB color images of the retina and ten of them contain pathology. The images are captured by a TopCon TRV-50 fundus camera

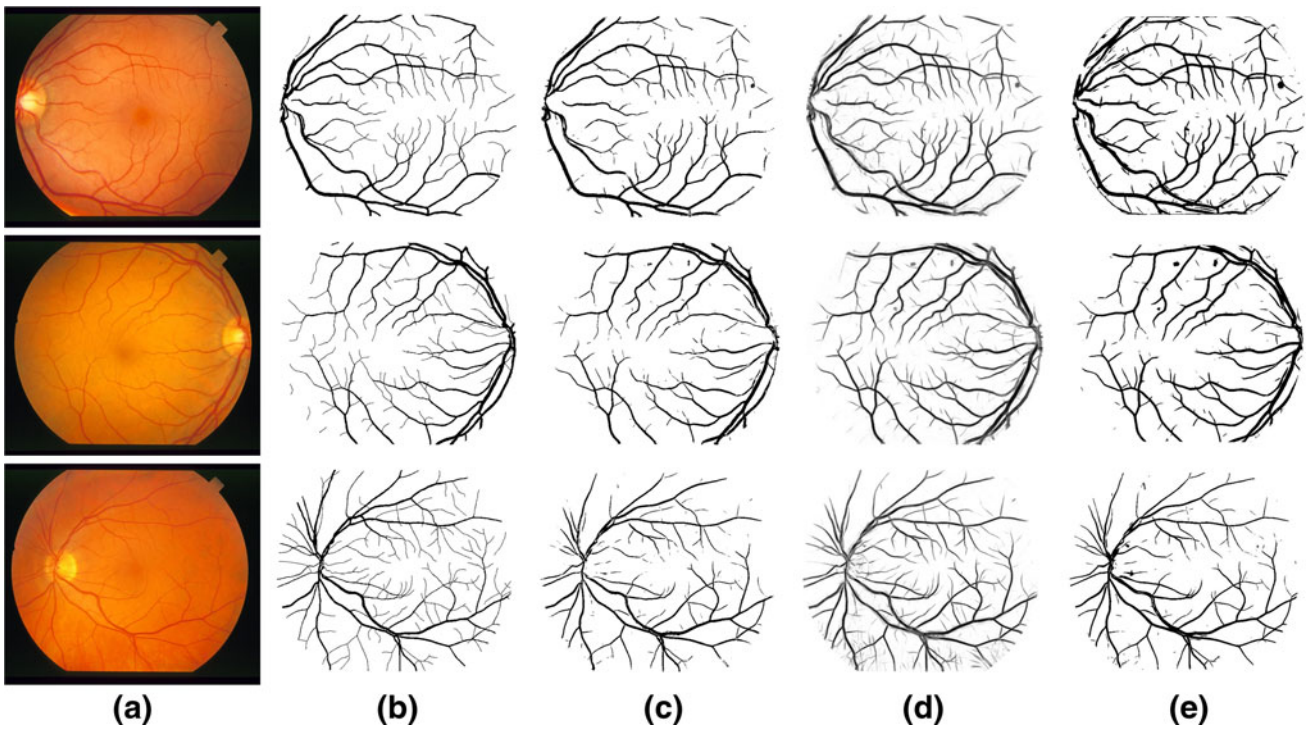

Fig. 8 Proposed technique results and manual segmentations (set A and set B) for three images from the STARE database: **a** original retinal images; **b** set A manual segmentation results; **c** set B manual segmentation results; **d** multilayered thresholding outputs; **e** segmentation results for proposed technique

with 35° FOV and the images are of size 605 × 700 pixels, 8 bits per color channel. Both retinal image datasets (DRIVE and STARE) are divided into a test and training set and each one contains half of the images. The test set is used for measurement of performance of the vessel segmentation algorithms. Two manually segmented hand labeling (set A and set B) are available for both databases made by two different human observers trained by an ophthalmologist. Figure 8 and Fig. 9 illustrate the blood vessel segmentation results for proposed method against manually segmented set A and set B for both STARE and DRIVE databases, respectively. Figure 10 compares the results of proposed segmentation technique against Hoover et al. [27] segmentation method.

The manually segmented images by first human observer are used as ground truth and the segmentations of set B are tested against set A, serving as a human observer reference for performance comparison truth [27, 28]. The performance of proposed technique is measured using receiver operating characteristic (ROC) curve which is a plot of true positive fraction versus false positive fraction. In order to find the accuracy and area under the ROC curve, following parameters are calculated.

- TP (true positive): Pixels that are computed as vessel pixels and they also belong to vessels in ground truth.
- FP (false positive): Pixels that are computed as vessel pixels but they are non-vessels in ground truth.
- TN (true negative): Pixels that are computed as non-vessel pixels and they are also non-vessels in ground truth.
- FN (false negative): Pixels that are computed as non-vessel pixels but they belong to vessels in ground truth.

Instead of using absolute values of above mentioned parameters, normally sensitivity and specificity are used and they are defined as following

$$\begin{aligned} \text{sensitivity} &= \frac{\text{TP}}{\text{TP}+\text{FN}} \\ \text{specificity} &= \frac{\text{FP}}{\text{TN}+\text{FP}}. \end{aligned} \tag{9}$$

True positive rate (TPR) is the fraction of number of true positive (pixels that actually belong to vessels) and total number of vessel pixels in the retinal image and false positive rate (FPR) is calculated by dividing false positives (pixels that don't belong to vessels) by total number of non-vessel pixels in the retinal image. Figure 11 shows the ROC curves for DRIVE and STARE databases produced using proposed method.

We compared the accuracy of proposed technique with Chaudhuri et al. [26], Jiang et al. [29], Staal et al. [21], Soares et al. [28] and Fraz et al. [30]. We also compared

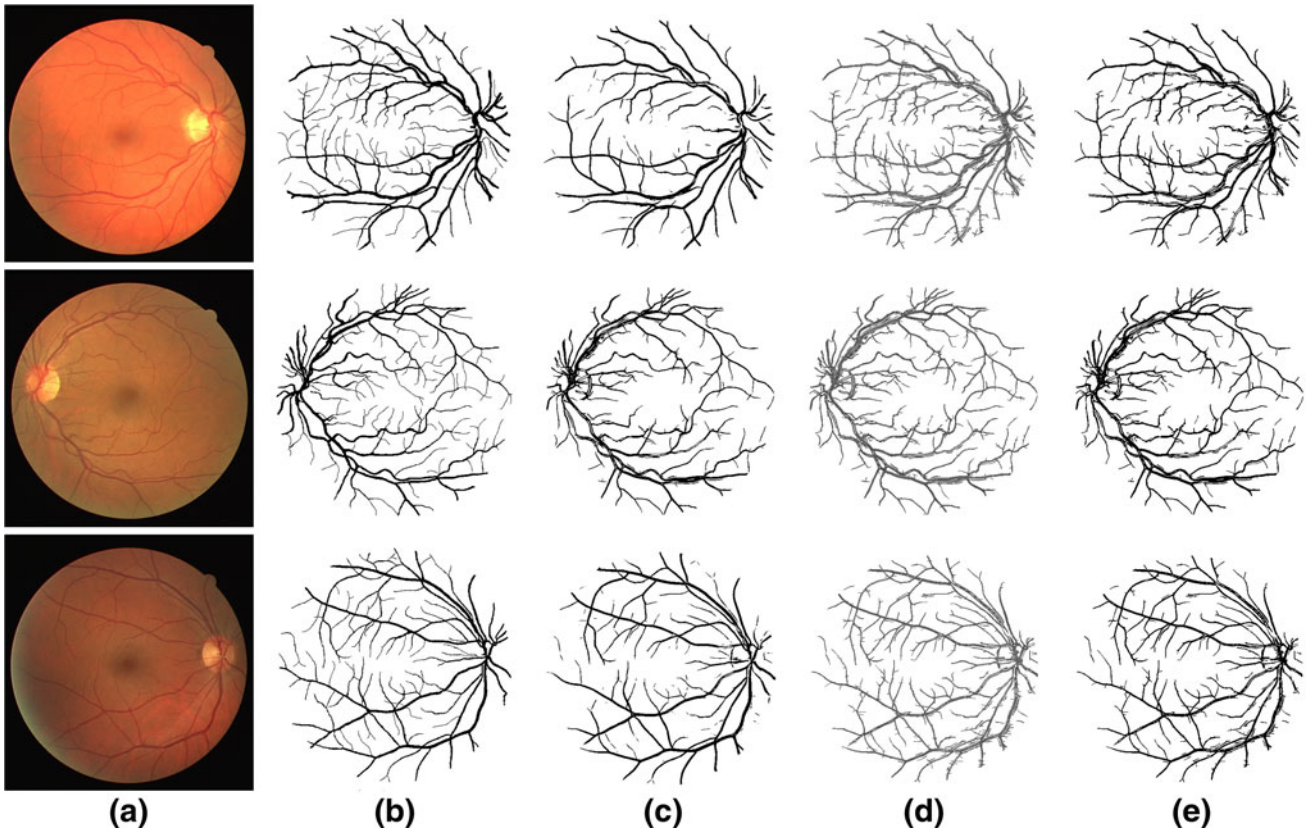

Fig. 9 Proposed technique results and manual segmentations (set A and set B) for three images from the DRIVE database: **a** original retinal images; **b** set A manual segmentation results; **c** set B manual segmentation results; **d** multilayered thresholding outputs; **e** segmentation results for proposed technique

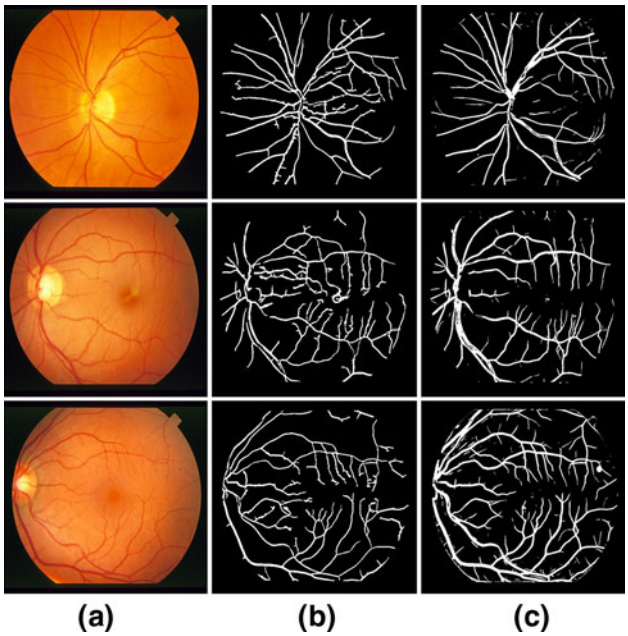

Fig. 10 Proposed technique results and Hoover et al. results for three images from the STARE database. **a** Original retinal images from STARE database; **b** results for Hoover et al. segmentation method; **c** segmentation results for proposed technique

our enhancement method with Hoover et al. [27]. Tables 2 and 3 summarize the results of vessel segmentation for DRIVE and STARE databases, respectively. They show the results in term of A_z and average accuracy for different segmentation methods compared with ground truth. A_z indicates the area under the ROC curve and accuracy is the fraction of pixels correctly classified. An accurate system that fully agreed with ground truth should have $A_z = 1$.

4 Conclusion

The appearance of blood vessels in retinal images plays an important role in diagnosis of many eye diseases. The proposed method segments the blood vessels from retinal images with great accuracy as compared to previous techniques. New multilayered thresholding-based approach for automated blood vessel segmentation is effective to handle vessel images under various conditions with reasonable accuracy and reliability for medical diagnosis. The problem with retinal images is that the visibility of vascular pattern is usually not good for thin vessels. So, it is necessary to enhance the vascular pattern. In this article,

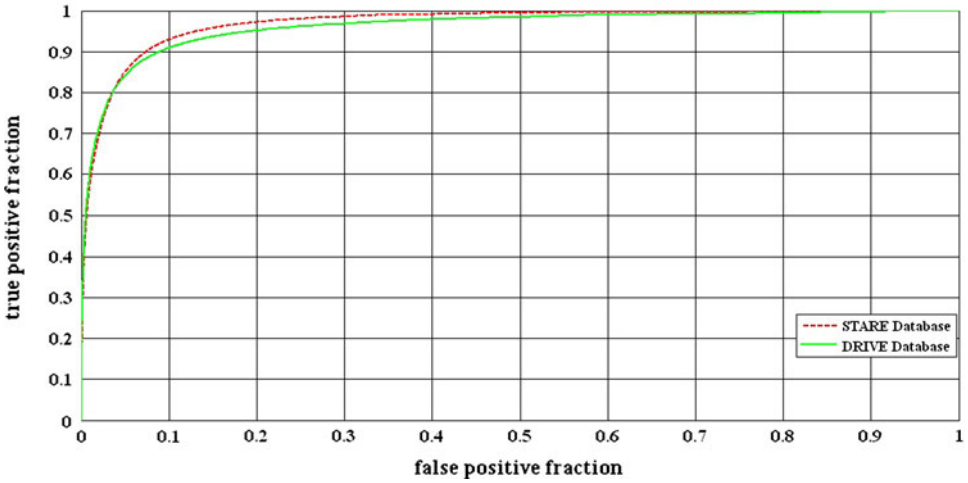

Fig. 11 ROC curves for STARE and DRIVE databases for proposed method

Table 2 Segmentation results I (DRIVE database)

Method	A_z	Accuracy
Chaudhuri et al.	0.9103	–
Jiang et al.	0.9327	0.8911
Staal et al.	0.9520	0.9441
Soares et al.	0.9614	0.9466
Bit plane slicing	–	0.9303
Proposed	0.9632	0.9469

Table 3 Segmentation results II (STARE database)

Method	A_z	Accuracy
Chaudhuri et al.	0.8987	–
Jiang et al.	0.9298	0.9009
Staal et al.	0.9614	0.9516
Soares et al.	0.9671	0.9480
Bit plane slicing	–	0.9367
Proposed	0.9706	0.9502

vessels are enhanced using 2-D Gabor wavelet. Vessel segmentation mask is created using multilayered thresholding technique which tracks vessel edges and check their connectivity by applying different thresholds iteratively. In addition, it eliminates all false edges and vessel segments prior to vessel tracking. The proposed technique is tested on publicly available DRIVE and STARE databases of manually labeled images. It is clear from the results section that the proposed method has outperformed previous well known methods in terms of accuracy and A_z. The presented method will be helpful in screening process of blood vessel for diagnosis of diabetic retinopathy as it has a high accuracy of detecting blood vessels.

Acknowledgments The authors would like to thank Hoover et. al. [27] and Staal et al. [21] for making their databases publicly available.

References

1. Susman EJ, Tsiaras WJ, Soper KA (1982) Diagnosis of diabetic eye disease. JAMA 247:3134–3231
2. Kanski J (1994) Clinical Opthalmology. Butterworh-Heinmann, London
3. Bhavsar AR (2002) Diabetic retinopathy, the diabetes eye exam initiative. Minn Med 85:46–47
4. Younis N, Broadbent DM, Harding SP, Vora JP (2002) Prevalence of diabetic eye disease in patients entering a systematic primary care-based eye screening programme. Diabet Med 19:1014–1021
5. Sinclair SH, Delvecchio C (2004) The internist's role in managing diabetic retinopathy: screening for early detection. Cleveland Clin J Med 71:151–159
6. Cavallereno J, Aiello LM (2005) Emerging trends in ocular telemedicine: the diabetic retinopathy model. J Telemed Telecare 11:163–166
7. Davis RM, Fowler S, Bellis K, Pocki J, Pakalnis VA, Woldorf A (2003) Telemedicine improves eye examination rates in individuals with diabetes. Diabetes Care 26:2476
8. Lightman S, Towler H (2003) Diabetic retinopathy. Clin Cornerstone 5:12–21
9. Martnez-Prez ME, Hughes AD, Thom SA, Bharath AA, Parker KH (1999) Retinal blood vessel segmentation by means of scale-space analysis and region growing. In: Medical image computing and computer-sssisted Intervention MICCAI, pp 90–97
10. Pinz A , Bernogger S, Datlinger P, Kruger A (1998) Mapping the human retina. IEEE Trans Med Imag 17:606–619
11. Tsai CL, Stewart CV, Tanenbaum HL, Roysam B (2004) Modelbased method for improving the accuracy and repeatability of estimating vascular bifurcations and crossovers from retinal fundus images. IEEE Trans Inf Technol Biomed 8:122–130
12. Foracchia M, Grisam E, Ruggeri A (2004) Detection of the optic disc in retinal images by means of a geometrical model of vessel structure. IEEE Trans Med Imag 23:1189–1195
13. Li H, Chutatape O (2004) Automated feature extraction in color retinal images by a model based Approach. IEEE Trans Biomed Eng 51:246–254

14. Mendona M, Campilho AJ (2006) Segmentation of Retinal Blood Vessels by Combining the Detection of Centerlines and Morphological Reconstruction. IEEE Trans Med Imag 25:1200–1213
15. Liu I , Sun Y (1993) Recursive tracking of vascular networks in angiograms based on the detection–deletion scheme. IEEE Trans Med Imag 12:334–341
16. Zhou L, Rzeszotarski MS, Singerman LJ, Chokreff JM (1994) The detection and quantification of retinopathy using digital angiograms. IEEE Trans Med Imag 13:619–626
17. Chutatape O, Zheng L, Krishnan SM (1998) Retinal blood vessel detection and tracking by matched Gaussian and Kalman filters. In: 20th Annual International Conference of the IEEE Engineering in Medicine and Biology Society (EMBS98), pp 3144–3149
18. Tolias YA, Panas SM (1998) A fuzzy vessel tracking algorithm for retinal images based on fuzzy clustering. IEEE Trans Med Imag 17:263–273
19. Can A, Shen H, Turner JN, Tanenbaum HL, Roysam B (1999) Rapid automated tracing and feature extraction from retinal fundus images using direct exploratory algorithms. IEEE Trans Inf Technol Biomed 3:125–138
20. Lalonde M, Gagnon L, Boucher M-C (2000) Non-recursive paired tracking for vessel extraction from retinal images. In: Vision Interface, pp 61–68
21. Staal J, Abramoff MD, Niemeijer M, Viergever MA, van Ginneken B (2004) Ridge-based vessel segmentation in color images of the retina. IEEE Trans Med Imag 23:501–509
22. McInerney T, Terzopoulos D (2000) T-snakes: Topology adaptive snakes. Med Image Anal 4:73–91
23. Toledo R, Orriols X, Binefa X, Radeva P, Vitri J, Villanueva J (2000) Tracking of elongated structures using statistical snakes. In: IEEE Computer Society Conference on Computer Vision and Pattern Recognition (CVPR), pp 157–162
24. Vasilevskiy A, Siddiqi K (2002) Flux maximizing geometric flows. IEEE Trans Pattern Anal Mach Intell 24:1565–1578
25. Nain D, Yezzi A, Turk G (2004) Vessel segmentation using a shape driven flow. In: Medical image computing and computer-assisted intervention MICCAI, pp 51–59
26. Chaudhuri S, Chatterjee S, Katz N, Nelson M, Goldbaum M (1989) Detection of blood vessels in retinal images using two dimensional matched filters. IEEE Trans Med Imag 8:263–269
27. Hoover A, Kouznetsova V, Goldbaum M (2000) Locating blood vessels in retinal images by piecewise threshold probing of a matched filter response. IEEE Trans Med Imag 19:203–211
28. Soares JVB, Leandro JJG, Cesar RM, Jelinek HF, Cree MJ (2006) Retinal vessel segmentation using the 2-D Gabor wavelet and supervised classification. IEEE Trans on Med Imag 25:1214–1222
29. Jiang X, Mojon D (2003) Adaptive local thresholding by verificationbased multithreshold probing with application to vessel detection in retinal images. IEEE Trans Pattern Anal Mach Intell 25:131–137
30. Fraz MM, Basit A, Javed MY (2008) Evaluation of retinal vessel segmentation methodologies based on combination of vessel centerlines and morphological processing. In: IEEE ICET08, pp 232–236
31. Antoine JP, Carette P, Murenzi R, Piette B (1993) Image analysis with two-dimensional continuous wavelet transform. Signal Process 31:241–272
32. Gonzalez RC, Woods RE (2002) Digital image processing. 2nd edn. Prentice hall, New Jersey